Evaluation of the contamination of the subsurface and groundwater by monoaromatic hydrocarbons in an eastern Amazonian town in northern Brazil

Karen Gomes
  Universidade Federal do Pará: Universidade Federal do Para

Pedro Oliva (✉ chira@ufpa.br)
  Universidade Federal do Para - Campus Braganca   https://orcid.org/0000-0002-3672-1577

Herson Rocha
  Universidade Federal Rural da Amazônia: Universidade Federal Rural da Amazonia

Rosivaldo Mendes
  Evandro Chagas Institute: Instituto Evandro Chagas

Amilton Costa
  Evandro Chagas Institute: Instituto Evandro Chagas

Camila Miranda
  Instituto Federal de Educacao Ciencia e Tecnologia do Para

Nelise Almeida
  Universidade Federal do Pará: Universidade Federal do Para

Abstract

When the underground storage tanks of gas stations leak fuel, the underlying substrate and groundwater may be contaminated by the monoaromatic hydrocarbons Benzene, Toluene, Ethylbenzene, and Xylene (BTEX). In this preliminary study, we used Ground Penetrating Radar (GPR) to detect possible plumes of contamination by hydrocarbons in the subsurface of gas stations in the Amazonian town of Bragança. The findings of this survey were complemented with Gas Chromatography/Mass Spectrometry (GC/MS), which was used to diagnose the presence of BTEX in water samples collected from the gas stations. At two stations, low electromagnetic signal reflections, which are caused by the lower permittivity of the gas vapor relative to water, were recorded in the vadose zone. Four water samples collected from the gas stations and local residences contained toluene, xylene or benzene. Toluene was detected in three of these samples, two from December 2017 (0.26 and 0.13 µg L^{-1}), and one from December 2018 (10.390 µg L^{-1}). Xylene was found in two samples from December 2017 (0.46 and 0.34 µg L^{-1}), while benzene was detected in one sample from December 2018 (0.558 µg L^{-1}). None of these samples exceeded the Detection Limit (DL) for any of the other BTEX compounds, and none of the other 20 samples collected were above the DL for any BTEX. According to Brazilian legislation for BTEX in drinking water, none of the samples collected in the study were considered unusable as a source of drinking water. The fact that BTEX were only recorded during the dry season indicates the natural attenuation of these compounds through their biodegradation in the subsurface, in particular during the rainy season. The integrated approach adopted in the present study produced satisfactory results for the study of contamination in the subsurface of the gas stations surveyed.

Introduction

The contamination of the soil, air, and groundwater by liquids leaking from the underground storage tanks of gas stations can impact the environment and have irreversible effects on human health (Hilpert et al. 2015; Moschini et al. 2005). These liquids may include fuel, toxic chemicals, and diluted effluents.

The underground storage tanks of gas stations represent a potential source of contamination, with the type and level of risk depending on the management of the stored fuel and the structural characteristics (e.g., type of soil, drainage) of the local landscape (Moschini et al. 2005). The spillage of hydrocarbon compounds may involve the contamination of the vadose and transition zones (the capillary fringe), which overlie the water table, by Light Non-Aqueous Phase Liquids (LNAPLs). Below the water table, contamination is by Dense Non-Aqueous Phase Liquids (DNAPLs). Hydrocarbons, such as gasoline, kerosene, and jet fuel, are common LNAPL contaminants (Jol 2009; Daniels et al. 1995; Domenico and Schwartz 1990).

The presence of NAPLs in the subsurface can be inferred by the fact that the contaminated groundwater and soils will have lower electrical conductivity and lower relative permittivity than the surrounding, uncontaminated matrix (Atekwana et al., 2000). The relative permittivity of hydrocarbons ranges from approximately 2 F m^{-1} to 30 F m^{-1}, compared with 80 F m^{-1} for water (Von Hippel 1961; Daniels et al.

1995), and the conductivity of hydrocarbons ranges from near 0 S m^{-1} to 0.02 S m^{-1} at frequencies of between 100 MHz and 1000 MHz (Von Hippel 1961; Daniels et al. 1995).

Environmental pollution by the monoaromatic hydrocarbons Benzene, Toluene, Ethylbenzene, and Xylene (BTEX) is a widespread phenomenon. Human exposure to these compounds can lead to a number of health problems, including the induction of cancer, given that compounds such as benzene are classified by the World Health Organization (WHO) as potent carcinogens in humans (Singh et al. 2017; Hilpert et al. 2015; Weelink et al. 2010; Badham and Winn 2007).

Hydrocarbon plumes may be delineated as areas of low resistivity if inorganic compounds are added to the contaminated groundwater for bioremediation. This will tend to increase the total amount of dissolved solids found in the subsurface (Benson et al. 1997; Asquith and Gibson 1982).

Geophysical techniques (e.g., electrical resistivity tomography (ERT), induced polarization (IP), Ground Penetrating Radar (GPR), and spontaneous potential, or SP) have been applied increasingly to the investigation, description, and monitoring of areas contaminated by hydrocarbons (Biosca et al. 2020).

The GPR signal provides a high-resolution image of the components of the plume, in particular in the vadose zone above the water table (Castro and Branco 2003). These authors detected the presence of LNAPLs in the vadose zone based on the presence of a zone of strongly-reduced reflections, and enhanced reflections in the contaminated transition and saturated zones. They concluded that the saturated zone became more reflective due to the presence of hydrocarbons dissolved in water.

The present study investigated possible contamination by gas stations in the town of Bragança, in eastern Brazilian Amazonia. The data were collected in the vicinity of the town's gas stations to identify possible plumes of contamination by hydrocarbon compounds in the subsurface. For this, the GPR was used in combination with Gas Chromatography/Mass Spectrometry to verify the possible contamination by BTEX in samples of groundwater collected near the gas stations. These methods were chosen for the present study due to their application in the diagnosis of contamination by hydrocarbons, rapid and non-destructive procedures and their relatively low cost.

Material And Methods

The present study was based on the combination of an indirect investigation method, that is, Ground-Penetrating Radar (GPR) and the direct analytical techniques of Gas Chromatography/Mass Spectrometry (GC/MS).

Study area

The study area is located in the town of Bragança in Pará state, northern Brazil (01°03'15" S, 46°46'10" W) which is located at an altitude of 19 meters above sea level (Fig. 1). According to IBGE (2022) the municipality has an area of 2.124,734 km^2, with an estimated population of 130,122 residents by 2021.

The Bragança microregion (Pará), in which the study area is located, was established on the local Neogene deposits. The basement of the coastal plain is composed of Tertiary sediments of the Barreiras Group (Fig. 2), which forms the Coastal Plateau (Souza Filho and El Robrini 1996). This area is part of the Amazon coast, which extends from the mouth of the Oiapoque River, in the Brazilian state of Amapá, to the eastern extreme of Maranhão state. Bragança is located at the mouth of the Caeté River.

Geologically, the Bragança coastal plain is located within the Bragança-Viseu coastal basin, whose origin and evolution are closely linked to the formation of the equatorial Atlantic and the normal faults that permeate the current coastal zone (Souza-Filho and El-Robrini 1996). The geomorphology of this coastal plain has changed significantly in recent years, with the retraction of the mangroves from the coast, due primarily to the encroachment of the sand that covers the muddy substrates of the mangrove and asphyxiates the vegetation (Lara 2003).

The geometry and paleogeography of the region are associated with tectonic processes, which determined the thickness of the local tertiary and quaternary deposits. The Tertiary is represented in the study area by the Pirabas (Góes et al. 1990) and Barreiras formations (Rossetti et al. 2001), while the Quaternary is represented by sandy-clay sediments and Holocene deposits of the alluvial, estuarine, and coastal plains (Souza Filho et al. 2009) (Fig. 2).

The study area has a very humid, megathermic climate, with moderate water deficiency between July and December. Temperatures vary only discreetly over the course of the year, ranging from a minimum of 18°C to a maximum of 33°C, with an annual mean of 27°C, and generally higher values between August and October. The region is dominated by the trade winds, primarily northeasterlies (with some shifts to the north and east), which are constant and moderate, with a maximum velocity of up to 7.5 m s^{-1} (Sousa Jr. et al. 2020; INMET 2020).

The climate of Pará state has two seasons, one rainy and the other, less rainy (or dry). The rainy season normally extends between January and May, while the dry season is from June to December (Magalhães et al. 2006). Precipitation in the rainy season ranges from 65 mm to 2744 mm, with a general mean of 1657 mm. In the dry season, precipitation ranges from 230 mm to 678 mm, with a mean of 487 mm (Moraes et al. 2005).

Ground Penetrating Radar (GPR)

We acquired GPR data in order to detect possible contamination plumes caused by hydrocarbons in the subsurface of the study area. Many previous studies have shown that GPR is an adequate geophysical tool for the detection of contaminated environments (e.g., Bacha et al. 2021; Aktürk and Doyuran 2015; Jiang et al. 2012; Castro and Branco 2003; Atekwana et al. 2000).

Six gas stations, identified as P01–P06 (Fig. 1), were surveyed in the present study, with a total of 24 water samples also being collected at the different sites.

Ground-Penetrating Radar uses electromagnetic (radio) waves of high frequency, that is 10–1000 MHz (Annan 1992), to survey underground structures. This geophysical tool is a non-invasive, versatile, and low-cost technique that can be used to survey an area rapidly, in both urban environments and areas of natural habitat. Ground-Penetrating Radar has many geological applications, such as the high-resolution imaging of shallow soils and rock structures, the identification of buried conduits and cavities, the mapping of the water table, and archeology and forensic investigations. When deployed, a short pulse of radar in the 10–1000 MHz frequency range is introduced into the subsurface, with the velocity of the radar by controlled by the dielectric constant and the conductivity of the subsurface (Kearey et al. 2002).

The GPR data were collected at each gas station in both the rainy and the dry seasons of 2017 and 2018. The data were acquired using a GSSI SIR-3000 system, with a 400 MHz antenna and time windows of 100, 150, and 200 nanoseconds (ns).

The system used for the acquisition of the electromagnetic signal was bi-static, with the common-offset (CO) configuration between the transmitting and receiving antennas. The GPR data were processed using the Reflexw software. We applied the following processing sequence (Delgado et al. 2022; Bacha et al. 2021; Sandmeier 2018; Annan 1996): edition of the profile orientation, static correction of zero-time, gain-energy decay, temporal filtering (band-pass), dewow filter, running average, background removal, and time-to-depth conversion. The hyperbola overlap method was used to determine the propagation velocity, and the time-depth conversion was based on a velocity of 0.09 m ns^{-1}.

Collection of water samples

Samples of groundwater were collected at each gas station and in the surrounding area in the rainy and dry seasons of 2017 and 2018. A total of 24 water samples were collected for the analysis of volatile organic compounds (BTEX). The samples were obtained from boreholes at the gas station sites and in adjacent residential areas. Informal interviews with local well diggers and the SIAGAS (2020) database confirmed that in general the water table of the study area is located at a depth of 6–10 m or < 6 m.

All the collection points had a faucet installed. The faucet was first opened to drain for 2–3 minutes or long enough to eliminate the stagnant water in the pipe. The faucet was then disinfected by applying a sodium hypochlorite solution (100 mg L^{-1}), with the excess solution being removed prior to the collection of the samples. A 100-mL sample of the water was collected from each point in a sterilized glass bottle, which was sealed and stored 4 $^{\circ}$C, to avoid the volatilization of the hydrocarbons. These bottles were transported to the city of Belém, capital of the Brazilian state of Pará, for analysis at the Toxicology Laboratory of the Environment Sector (SAMAM) of the Evandro Chagas Institute/Brazilian Ministry of Health (IEC/SVS/MS).

The samples were collected and preserved in accordance with the methods established in the 21st edition of the Standard Methods for the Examination of Water and Wastewater, method SM-6010 B (APHA 2005), and the National Water Agency (ANA) of the Brazilian Ministry of the Environment (ANA 2011). The BTEX concentrations were determined by Gas Chromatography/Mass Spectrometry (GC/MS). Gas

Chromatography (GC) is a widely-used technique for the identification of hydrocarbons and the quantification of mixtures of organic compounds (Pavón et al., 2007, Côcco et al. 2005). To analyze water samples containing BTEX, GC is normally combined with others techniques, such as Mass Spectrometry, or MS (Lee et al. 2007; Pavón et al. 2007; Jochmann et al. 2006; Nakamura and Daishima 2005).

The BTEX values identified in the present study were compared with the Maximum Value Allowed (MVA) in drinking water under Brazilian legislation. The MVA for benzene in water destined for human consumption is 5 µg L^{-1}, while that of toluene is 30 µg L^{-1}, ethylbenzene is 300 µg L^{-1}, and xylene is 500 µg L^{-1}(BRASIL 2021).

Extraction of the BTEX from the water samples

The BTEX were extracted from the water samples using the automated Headspace (HS) method, which is based on the D 6040 method (Wallace and Stenerson 2008). Aliquots of 15 mL of the samples were placed in 20 mL bottles, sealed with an aluminum seal and teflon septum. The samples were then wrapped in aluminum blocks, placed in a Triplus RSH autosampler, and heated to 80°C for 10 minutes.

The composition of the samples was quantified using a Trace 1300 gas chromatograph (Thermo Scientific) coupled to a TSQ 8000 mass spectrometer (Thermo Scientific), using a TG-5MS column (Thermo Scientific) composed of 5% phenyl and 95% dimethylsiloxane, with 30 m x 0.32 mm x 0.25 µm film. The oven temperature of the column was maintained at 40°C for 1 minute, then raised to 70°C, at 5°C per minute, and finally to 70–220°C at 30°C per minute. The Detection Limits (DLs) considered here were 0.05 µg L^{-1} for benzene, ethylbenzene and xylene, and 0.1 µg L^{-1} for toluene.

The carrier gas was helium (99.999% pure) used at a flow rate of 1.0 ml min $^{-1}$. The injector was operated at 280°C in the split mode. The transfer line temperature was 250°C, and the ion source was present at 230°C. A 1000-µL aliquot of the sample contained in the headspace was injected into the chromatograph.

Results And Discussion

Two gas stations (P02 and P06) presented radargrams which had a region of attenuated reflections or low amplitudes in the vadose zone. The GPR profiles of station P02 were obtained from transects of between 10 m and 16 m in length, while at P06, the profiles were between 30 m and 43 m long. The electromagnetic signal was generated at 2 m intervals along the length of each profile.

At gas station P02, hyperbolic electromagnetic signals were identified parallel to the location of the fuel pumps in the radargrams of profile L1 (Fig. 3), which correspond to the storage tank caps. Hyperbolic electromagnetic signals corresponding to the storage tank caps were also identified in the radargrams of profile L3 (Fig. 4), which is perpendicular to L1, together with responses that correspond to the pipes in the ground in the vicinity of the fuel pumps. Hyperbolic electromagnetic signals were also identified in the radargrams obtained from profile L4 at gas station P06 (Fig. 5), which corresponded to the locations of

the storage tanks and pipes, as well as responses that correspond to the base of the support column of the gas station.

The radargrams collected during the dry season also revealed the presence of low amplitude zones and hyperbolic electromagnetic signals, indicating the location of the underground tanks and their connecting pipes (Figs. 3, 6 and 7). These areas of low reflection are located in close proximity to the storage tanks. Castro and Branco (2003) concluded that these features correspond to a hydrocarbon vapor phase in the vadose zone or the region between the surface and the water table, in which the pores in the rock are not completely filled with water.

Daniels et al. (1995) reported that these areas of low reflection may be attributed to the reduced plane wave reflection coefficients from unsaturated sand filled partially by the vapor phase of LNAPLs. Gas station P02 has been in operation for 33 years, and P06, for 31 years, which implies that the age of the tanks may be a key factor, given that corrosion and cracks tend to arise after 20 years of use (Blackman Jr 2001; Cole 1994).

Profile L2 (Fig. 6) was used to calculate the propagation velocity (0.081 m s^{-1}), the electrical conductivity (50 S m^{-1}), and the relative dielectric permittivity (13.8 F m^{-1}) of the saturated clayey soil, at depths of below 2−2.4 m in the saturated zone (Table 1). Profile L3 at station P06 (Fig. 7) was used to determine the physical properties of the organic contaminants in the low reflection zone, including the electromagnetic wave velocity (0.19 m s^{-1}), the electrical conductivity (0.27 S m^{-1}), and the dielectric permittivity (2.4 F m^{-1}) of the dry, clayey soil. Castro and Branco (2003) concluded that the attenuation of the GPR signal near the surface is due to the low permittivity of the hydrocarbon product (gas vapor) relative to water.

Table 1
Dielectric permittivity (ε), electrical conductivity (σ), and electromagnetic wave velocity (v) measured from the vadose and saturated zones.

Property	Vadose zone	Saturated zone
Dielectric permittivity (ε)	$2.4\,Fm^{-1}$	$13.8\,Fm^{-1}$
Electrical conductivity (σ)	$0.27\,Sm^{-1}$	$50\,Sm^{-1}$
Electromagnetic wave velocity (v)	$0.19\,ms^{-1}$	$0.081\,ms^{-1}$

The results of the GC-MS analyses of the groundwater samples collected during the present study are shown below. In December 2017 (Table 2), toluene and xylene were detected in the samples from gas station P01. In sample A01, toluene was present at a concentration of 0.26 µg L^{-1} and xylene at 0.46 µg L^{-1}. The same monoaromatic hydrocarbons were identified in sample A02 from the same gas station (P01), at concentrations of 0.13 µg L^{-1} (toluene) and 0.34 µg L^{-1} (xylene). All the other samples from this site presented values below the Detection Limit (< DL). While these concentrations are considerably higher than those recorded in any of the other samples collected during the present study, they are much lower

than those (MVA) defined by the Brazilian legislation for drinking water (BRASIL 2021). As gas station P01 has been in operation for 35 years, the age of the tanks may, once again, have provoked corrosion and cracks that would give rise to fuel leakage.

Table 2
Results of the analysis of BTEX in the water samples collected during the present study in Bragança, Pará, Brazil, in December 2017 (dry season).

Sample	Site	Benzene (µg L^{-1})	Toluene (µg L^{-1})	Ethylbenzene (µg L^{-1})	Xylene (µg L^{-1})
A01	Gas station P01	< DL	0.26	< DL	0.46
A02	Home near gas station P01	< DL	0.13	< DL	0.34
A03	Gas station P02	< DL	< DL	< DL	< DL
A04	Gas station P03	< DL	< DL	< DL	< DL
A05	Gas station P04	< DL	< DL	< DL	< DL
A06	Gas station P05	< DL	< DL	< DL	< DL
A07	Gas station P06	< DL	< DL	< DL	< DL
A08	Gas station store P06	< DL	< DL	< DL	< DL

Intrinsic bioremediation (natural attenuation) involves the application of endogenous microorganisms to degrade hazardous compounds, such as BTEX, present in aquifers (Corseuil and Alvarez 1996; Borden et al. 1995). The absence of BTEX concentrations higher than the MVA established by the Brazilian legislation (BRASIL 2021) indicates the occurrence of the natural attenuation of BTEX in the subsurface. It is nevertheless important to understand the factors that determine this process, and its potential risks to humans and the environment (Borden et al. 1995).

None of the samples collected in May (rainy season) 2018 exceeded the DL for any of the BTEX in the CG-MS analysis. Given this, none of the samples can be considered to be contaminated by these compounds.

Similar values (< DL) were also recorded in most of the samples collected in the dry season month of December 2018 (Table 3), although benzene was recorded in sample A02 (0.558 µg L^{-1}), from gas station P01, and toluene was found in sample A03 (10.390 µg L^{-1}), from gas station P02. All the other samples were below the Detection Limit (< DL). While these values are much higher than those recorded in December 2017, they are still well below the MVAs defined by Brazilian legislation (BRASIL 2021).

Table 3
Results of the analysis of BTEX in the water samples collected during the present study in Bragança, Pará, Brazil, in December 2018 (dry season).

Sample	Site	Benzene (µg L^{-1})	Toluene (µg L^{-1})	Ethylbenzene (µg L^{-1})	Xylene (µg L^{-1})
A01	Gas station P01	<DL	< DL	< DL	< DL
A02	Home near gas station P01	0.558	< DL	< DL	< DL
A03	Gas station P02	< DL	10.390	< DL	< DL
A04	Gas station P03	< DL	< DL	< DL	< DL
A05	Gas station P04	< DL	< DL	< DL	< DL
A06	Gas station P05	< DL	< DL	< DL	< DL
A07	Gas station P06	< DL	< DL	< DL	< DL
A08	Gas station store P06	< DL	< DL	< DL	< DL

All the samples collected in the rainy seasons of 2017 and 2018 were below the Detection Limit (< DL) for all the BTEX compounds. These findings may reflect a natural biodegradation process, provoked by a combination of intense rainfall and chemical reactions, through which the hydrocarbons may be transformed into electron acceptors and absorbed by microorganisms. Electron acceptors include oxygen, nitrate, iron oxides, water, and carbon dioxide (Borden et al. 1995; Weelink et al. 2010). Hydrocarbon compounds may disperse in the environment due to a number of processes, such as the drainage of intense precipitation and seasonal variations in the hydrological gradient (Daniels*et al.* 1995).

Conclusions

The GPR data permitted the identification of the presence of low-amplitude reflections in the vadose zone of two gas stations (P02 and P06) whose attenuation near the surface was due to the low permittivity recorded in the radargrams, which may be caused by the reduced permittivity of the hydrocarbon products (gas vapor) in comparison with water.

Water samples collected from boreholes located in the gas stations and adjacent areas were analyzed for the presence contamination by BTEX and identified toluene, xylene and benzene at two sites (P01 and P02) in the dry season, although the concentrations were very low and no problematic loss of water quality was detected, given that the values detected were all within the Brazilian Health Ministry thresholds for the presence of BTEXs in drinking water. The presence of these contaminants in the dry

season is nevertheless worrisome, and highlights the need for further monitoring, given the potential risks of exposure of both employees and local residents to BTEXs at the contaminated sites.

As there are no programs in place locally for the remediation of the contamination of the soil or water sources, it seems likely that the low BTEX concentrations identified in the present study are the result of a process of natural attenuation, in particular during the rainy season. Further research would be essential, however, to better determine the potential mechanisms of natural attenuation. Monitoring is both necessary and recommendable, to better determine the status of the subsurface of the gas stations and adjacent areas and, in particular, the detection of possible shifts in the levels of contamination of the sites at which BTEXs were detected. Overall, the integrated approach adopted in the present study (GPR + CG/MS) proved effective for the complementary study of the contamination in the subsurface of the gas stations in the study area.

Declarations

Conflict of interest The authors declare that they have no conflict of interest.

Ethical approval This article does not contain any studies with animals performed by any of the authors.

References

1. Aktürk O, Doyuran V (2015) Integration of electrical resistivity imaging (ERI) and ground penetrating radar (GPR) methods to identify soil profile around Necatibey Subway Station, Ankara, Turkey. Environ Earth Sci 74(3):2197-2208. https://doi.org/10.1007/s12665-015-4211-3

2. Annan AP (1996). Transmission dispersion and GPR. J. Environ. Eng. Geophys. 2, 125–136. https://doi:10.4133/jeeg1.b.125

3. Annan AP (1992) Ground Penetration Radar Workshop Notes. Sensors & Software, Inc., Internal Report.

4. APHA (2005) Standard methods for the examination of water and wastewater. American Public Health Association, American Water Works Association and Water Environment Federation, Washington DC

5. ANA (2011) Agência Nacional de Águas - Ministério do Meio Ambiente. Companhia Ambiental do Estado de São Paulo. Guia nacional de coleta e preservação de amostras: água, sedimento, comunidades aquáticas e efluentes líquidas. Brasília, 326 p. Available online:

<https://cetesb.sp.gov.br/wp-content/uploads/2021/10/Guia-nacional-de-coleta-e-preservacao-de-amostras-2012.pdf>. Accessed on 06 February 2021.

6. Asquith GB, Gibson CR (1982) Basic well log analysis for geologists. American Association of Petroleum Geologists

7. Atekwana EA, Sauck WA, Werkema, DD (2000) Investigations of geoelectrical signature at a hydrocarbon contaminated site. J Appl Geophys 44:167-180. https://doi.org/10.1016/S0926-9851(98)00033-0

8. Bacha D de CS, Santos S, Mendes R de A, Rocha CCH da S, Corrêa JA, Cruz JCR, Abrunhosa FA, Oliva PAC (2021) Evaluation of the contamination of the soil and water of an open dump in the Amazon Region, Brazil. Environ Earth Sci 80:1-12. https://doi.org/10.1007/s12665-021-09401-3

9. Badham HJ, Winn, LM (2007) Investigating the role of the aryl hydrocarbon receptor in benzene-initiated toxicity in vitro. Toxicology 229: 177-185. https://doi.org/10.1016/j.tox.2006.10.021

10. Benson AK, Payne KL, Stubben MA (1997) Mapping groundwater contamination using dc resistivity and VLF geophysical methods - a case study. Geophysics 64:80-86. https://doi.org/10.1190/1.1444148

11. Biosca B, Arévalo-Lomas L, Barrio-Parra F, Díaz-Curiel J (2020) Application and limitations of time domain-induced polarization tomography for the detection of hydrocarbon pollutants in soils with electro-metallic components: a case study. Environmental Monitoring and Assessment 192: 115. https://doi.org/10.1007/s10661-020-8073-0

12. Blackman Jr, WC (2001) Basic Hazardous Waste Management. 3rd ed., Florida, USA, Lewis Publishers.

13. Borden RC, Gomez CA, Becker MT (1995) Geochemical indicators of intrinsic bioremediation. Groundwater 33: 180-189.

14. BRASIL (2021) Ministério da Saúde. Portaria no. 888, de 04 de maio de 2021. Dispõe sobre a alteração do Anexo XX da Portaria de Consolidação GM/MS nº 5, de 28 de setembro de 2017, para dispor sobre os procedimentos de controle e de vigilância da qualidade da água para consumo humano e seu padrão de potabilidade. Available online:< https://www.in.gov.br/en/web/dou/-/portaria-gm/ms-n-888-de-4-de-maio-de-2021-318461562>. Accessed on 07 February 2022.

15. Castro DL, Branco RMGC (2003) 4-D ground penetrating radar monitoring of a hydrocarbon leakage site in Fortaleza (Brazil) during its remediation process: a case history. Journal of Applied Geophysics 54: 127-144. https://doi.org/10.1016/j.jappgeo.2003.08.021

16. Côcco LC, Yamamoto CI, Von Meien OF (2005) Study of correlations for physicochemical properties for Brazilian gasoline. Chemometrics and intelligent laboratory systems 76:55-63. https://doi.org/10.1016/j.chemolab.2004.09.004

17. Cole GM (1994) Assessment and Remediation of Petroleum Contaminated Sites. Florida, USA, Lewis Publishers.

18. Corseuil HX, Alvarez PJJ (1996) Natural bioremediation perspective for BTX-contaminated groundwater in Brazil: effect of ethanol. Water Science and Technology 34: 311-318. https://doi.org/10.1016/S0273-1223(96)00759-7

19. Daniels JJ, Roberts R, Vendl, MA (1995) Ground Penetrating Radar for the detection of liquid contaminants. Journal of Applied Geophysics 33: 195-207. https://doi.org/10.1016/0926-9851(95)90041-1

20. Delgado LFS, Oliva PAC, El Robrini M, Reis Júnior JA dos (2022) Contribution of Ground Penetrating Radar in the study of an amazon tide channel, influenced by macro tide. Journal of South American Earth Sciences 116 (103776), 1-12. https://doi.org/10.1016/j.jsames.2022.103776

21. Domenico PA, Schwartz FW (1990) Physical and chemical Hydrogeology. Wiley, New York

22. Góes AM, Rossetti DF, Nogueira ACR, Toledo PM (1990) Preliminary depositional model of the Pirabas Formation in the northeast of the State of Pará (in Portuguese). Boletim do Museu Paraense Emílio Goeldi, Série Ciências da Terra 2: 3-15

23. Google Earth Pro (2022) Computer program. https://www.google.com/earth/versions/

24. Hilpert M, Mora BA, Ni J, Rule AM, Nachman KE (2015) Hydrocarbon Release During Fuel Storage and Transfer at Gas stations: Environmental and Health Effects. Current Environmental Health Reports 2: 412-422. https://doi.org/10.1007/s40572-015-0074-8

25. IBGE (2022) Instituto Brasileiro de Geografia e Estatística. Cidades e Estados. Available online: <https://www.ibge.gov.br/cidades-e-estados/pa/braganca.html> Accessed on 15 March 2022.

26. IBGE (2015) Instituto Brasileiro de Geografia e Estatística. Bases e Referenciais: bases cartográficas: malhas digitais. Ano de referência 2015. Available online: < https://mapas.ibge.gov.br/bases-e-referenciais/bases-cartograficas/malhas-digitais.html> Accessed on 01 July 2019.

27. INMET (2020) Instituto Nacional de Meteorologia - Ministério da Agricultura, Pecuária e Abastecimento, Brasil. Available online <https://portal.inmet.gov.br/>. Accessed on 15 March 2020.

28. Jiang Y, Li Y, Kang X, Zhou Q, Zhou X, Zhu Y (2012) Characteristics of Leakage Pollution of Longpan Road Gas station and Its Enlightenment. Journal of Environmental Protection 3:49-54. https://doi.org/10.4236/jep.2012.31006

29. Jochmann MA, Kmiecik MP, Schmidt TC (2006) Solid-phase dynamic extraction for the enrichment of polar volatile organic compounds from water. Journal of Chromatography A 1115:208-216. https://doi.org/10.1016/j.chroma.2006.02.061

30. Jol HM (ed.) (2009) Ground Penetrating Radar: Theory and Applications. Elsevier Science, Amsterdam, The Netherlands. First Edition.

31. Jorge MVE (2017) Geological-Geophysical Framework of the Northeast Region of the State of Pará (in Portuguese). Dissertation. Federal University of Pará. Institute of Geosciences. Postgraduate Program in Water Resources. Available online:< http://repositorio.ufpa.br/jspui/handle/2011/10754>. Accessed on 07 February 2022.

32. Kearey P, Brooks M, Hill I (2002) An Introduction to Geophysical Exploration. Blackwell Science Ltd.

33. Lara RJ (2003) Amazonian mangroves - a multidisciplinary case study in Pará State, North Brazil: introduction. Wetlands Ecology and Management 11: 217-221.

34. Lee M-R, Chang Ch-M, Dou J (2007) Determination of benzene, toluene, ethylbenzene, xylenes in water at sub-ng l1 levels by solid-phase microextraction coupled to cryo-trap gas chromatography–mass spectrometry. Chemosphere 69:1381-1387. https://doi.org/10.1016/j.chemosphere.2007.05.004

35. Magalhães A, Costa RM, Liang TH, Pereira LCC, Ribeiro MJS (2006) Spatial and temporal distribution in density and biomass of two *Pseudodiaptomus* Species (COPEPODA: CALANOIDA) in the Caeté river estuary (Amazon region - north of Brazil). Braz. J. Biol., 66: 421-430.

36. Moraes BC de, Costa JMN da, Costa ACL da, Costa MH (2005) Spatial and temporal variation of precipitation in the state of Pará. Acta Amazonica 35: 207-214. https://doi.org/10.1590/S0044-59672005000200010 (in Portuguese)

37. Moschini LE, Santos JE dos, Pires JSR (2005) Environmental diagnosis of risk areas related to gas stations. Brazilian Archives of Biology and Technology 48: 657-666. https://doi.org/10.1590/S1516-89132005000500019

38. Nakamura S, Daishima S (2005) Simultaneous determination of 22 volatile organic compounds, methyl-tert-butyl ether, 1,4-dioxane, 2-methylisoborneol and geosmin in water by headspace solid phase microextraction-gas chromatography–mass spectrometry. Analytica Chimica Acta 548(1-2):79-85. https://doi.org/10.1016/j.aca.2005.05.077

39. Pavón JLP, Sánchez M del N, Laespada MEF, Cordero BM (2007) Simultaneous determination of gasoline oxygenates and benzene, toluene, ethylbenzene and xylene in water samples using headspace-programmed temperature vaporization-fast gas chromatography–mass spectrometry. Journal of Chromatography A 1175: 106-111. https://doi.org/10.1016/j.chroma.2007.10.044

40. Rossetti DF, Góes AM, Souza LSB (2001) Stratigraphy of the Pós-Barreiras sedimentary succession (Bragantine Zone, Pará) based on ground penetrating radar. Revista Brasileira de Geofísica 19: 113-130. https://doi.org/10.1590/S0102-261X2001000200001

41. Sandmeier KJ (2018) ReflexW manual, version 8.5. Program for the Processing of Seismic, Acoustic or Electromagnetic Reflection, Refraction and Transmission Data. Karlsruhe, Germany, 652 p.

42. SIAGAS (2020) Groundwater Information System. SIAGAS-CPRM/Geological Survey of Brazil (SGB). Available online: <http://siagasweb.cprm.gov.br/layout/index.php> Accessed on 12 January 2021.

43. Singh P, Jain R, Srivastava N, Borthakur A, Pal DB, Singh R, Madhav S, Srivastava P, Tiwary D, Mishra PK (2017) Current and emerging trends in bioremediation of petrochemical waste: A review. Critical Reviews in Environmental Science and Technology 47: 155-201. https://doi.org/10.1080/10643389.2017.1318616

44. Sousa Júnior, CN da C, El Robrini, M, Oliva, PACh (2020) Experimental survey of the Ground Penetrating Radar (GPR) in the study of the Aturiaí river (Bragança Coastal Plain, northeast of Pará) (In Portuguese). Research, Society and Development 9: 1-29. http://dx.doi.org/10.33448/rsd-v9i10.8821

45. Souza Filho PWM, EL-Robrini M (1996) The morphology, sedimentation processes and lithofacies of the morpho-sedimentary environments of the Bragantine coastal plain - northeast of the state of Pará (Brazil) (In Portuguese). Geonomos 4: 1-16. https://doi.org/10.18285/geonomos.v4i2.197

46. Souza Filho PWM, Lessa GC, Cohen MCL, Costa FR, Lara RJ (2009) The Subsiding Macrotidal Barrier Estuarine System of the Eastern Amazon Coast, Northern Brazil. In: Geology and Geomorphology of Holocene Coastal Barriers of Brazil. Lecture Notes in Earth Sciences 107: 347–375. https://doi.org/10.1007/978-3-540-44771-9_11

47. Von Hippel AR (Ed.) (1961) Dielectric Materials and Applications. MIT Press, Cambridge, MA

48. Wallace R, Stenerson K (2008) Method 6040D, Odors in Drinking Water, Using SPME on the Supelco SLB-5ms Capillary Column. The Application Notebook. https://www.chromatographyonline.com/view/method-6040d-odors-drinking-water-using-spme-supelco-slb-5ms-capillary-column. Accessed 13 January 2022.

49. Weelink, SAB, Van Eekert, MHA, Stams, AJM (2010) Degradation of BTEX by anaerobic bacteria: physiology and application. Reviews in Environmental Science and Bio/Technology 9: 359-385. https://doi.org/10.1007/s11157-010-9219-2

Figures

Figure 1

Study area and the location of the gas stations (red circles) surveyed in the town of Bragança (Pará, Brazil). Adapted and modified from IBGE (2015) and Google Earth Pro (2022).

Figure 2

Geological map of northeastern Pará state (Brazil), showing the study area (Bragança, Brazil). Source: Jorge (2017).

Figure 3

Radargrams obtained from profile L1 at gas station P02 in (A) April 2018 and (B) December 2018.
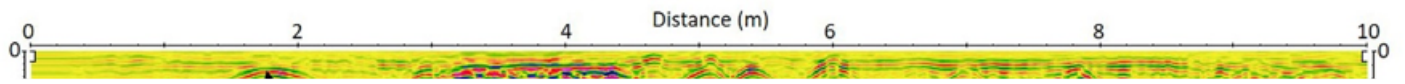
Figure 4

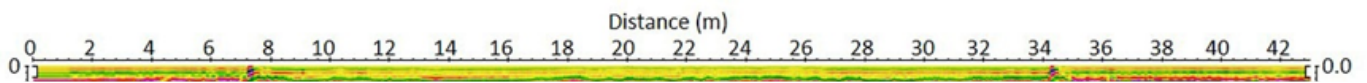Radargram obtained from profile L3 at gas station P02 in December 2017.

Figure 5

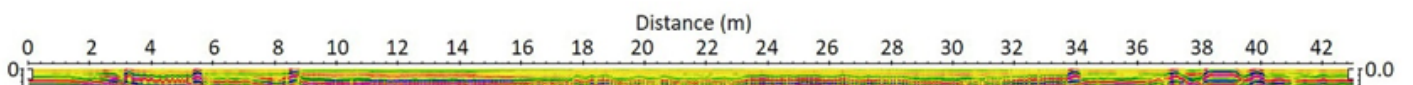Radargram obtained from profile L4 at gas station P06 in December 2017.

Figure 6

Radargrams obtained from profile L2 at gas station P06 in December 2017.
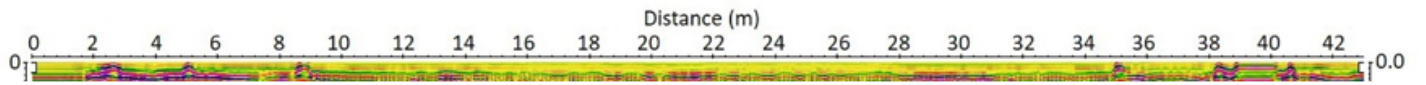
Figure 7

Radargrams obtained from profile L3 at gas station P06 in December 2017.